Journal of Magnetic Resonance **138,** 36–42 (1999)
Article ID jmre.1999.1730, available online at http://www.idealibrary.com on IDEAL®

An NMR Relaxation Study of the State of Water in Gelatin Gels

Marie-Claire Vackier,* Brian P. Hills,† and Douglas N. Rutledge*

*Institut National Agronomique Paris-Grignon, Laboratoire de Chimie Analytique, 16 rue Claude Bernard, 75231 Paris Cedex 05, France; and †Institute of Food Research, Norwich Research Park, Colney, Norwich NR4 7UA, UK

Received February 27, 1998; revised January 20, 1999

A combination of ^{1}H and ^{23}Na NMR is used to probe the dynamic state of water in gelatine gels as the water content is lowered from 70% to dryness. A sharp increase in the proton and sodium transverse relaxation rates is observed as the water content falls from 20 to 15% while the proton longitudinal and dipolar cross relaxation rates show a maximum at ca. 15%. We show that these observations can be understood if monolayer coverage occurs at 15% and multilayers of less strongly interacting hydration water are formed between 15 and 20%. Above 20% the water appears to behave as an unperturbed bulk phase. © 1999 Academic Press

Key Words: **time domain nuclear magnetic resonance; relaxation time; correlation time; matrix mobilization; cross-relaxation.**

INTRODUCTION

Water plays an important role in foods because of its influence on mechanical and rheological properties and its effect on the rates of chemical, enzymatic, and microbial spoilage reactions that limit food shelflife. Of the many techniques that can be used to study water–biopolymer interactions in foods, NMR is unique in that, depending on the choice of pulse sequence, it can probe the dynamic states of both the water and the biopolymer on a variety of time scales. Several high-resolution NMR studies on dilute aqueous solutions of low molecular weight proteins have shown that, by combining relaxation time and NOE measurements, it is possible to build a detailed picture of the dynamics of water–biopolymer interactions; several well-characterized examples now exist in the literature (*1, 2*). Attempts to extend these studies to more concentrated biopolymer solutions eventually fail because polymer entanglement reduces the transverse relaxation time and broadens the spectral lines. For this reason low water content biopolymer systems are preferably studied by multinuclear relaxation dispersion techniques. Proton and deuterium relaxation is complicated by the existence of chemical exchange between the water and biopolymer and, in the case of longitudinal proton magnetization, by dipolar cross relaxation. For this reason water oxygen-17 relaxation is the nucleus of choice and a number of oxygen-17 dispersion studies have been undertaken on concentrated sugar solutions (*3, 4*), protein (*5*), and polysaccharide systems (*6*). Unfortunately, the water oxygen-17 (and deuterium) relaxation times can become prohibitively short in very low water content systems, so, when this is the case one must resort to proton relaxation and suffer the possible interpretational complexities of proton exchange and dipolar cross relaxation.

Although proton relaxation has been studied in a number of diverse food-related materials (*7*), we have chosen to focus our low-water-content proton relaxation studies on gelatin gels. These gels give single exponential water proton transverse relaxation showing that our NMR relaxation measurements do not probe spatial heterogeneity in these gels. This is consistent with a structure based on a cross-linked network of protein chains showing no spatial heterogeneity above the macromolecular distance scale. Indeed, we have already successfully interpreted the dilute regime using the proton exchange cross-relaxation model (*8, 9*), which assumes spatial homogeneity above the macromolecular distance scale. In this paper we therefore extend the study to lower water contents which are relevant to a much wider range of real food materials.

Our earlier, preliminary studies of more concentrated gelatine systems (*9–12*) and of dried carrots (*13*) showed that the amount of a slowly relaxing proton pool (measured by the parameter $M0_{src}/FID_{11}$, described later) increases dramatically when the water content rises above about 20% (*12*). Assigning this slowly relaxing proton pool to particular chemical species is not straightforward. It is tempting to assume that below 20%, the water strongly interacts with the protein and is not available to solvate other molecular species. Only above this critical water content will water then become available to solubilize protein fragments derived from gelatin. Alternatively, it could be that water contents above 15–20% plasticize the gelatin gel network, in which case it is the mobility of the gel network itself that is being monitored. Yet another possibility is that proton exchange between the water and exchangeable gelatin proton pool only occurs at water contents exceeding 15–20% and is associated with an increase in the slow relaxing proton component. It should be pointed out that glassy transition phenomena cannot be responsible for the changes in relaxation behavior as the glass transition temperature, T_g, is so high for gelatin gels at these low water contents that it cannot be measured without degrading the gelatin.

Distinguishing these various possibilities is not straightfor-

1090-7807/99 $30.00
Copyright © 1999 by Academic Press
All rights of reproduction in any form reserved.

ward. If the first hypothesis is true, that water contents in excess of ca. 20% permit the dissolution of other, low molecular weight solutes, then there should also be a sharp increase in the mobility of ions such as sodium in gelatin-salt gels. For this reason we have supplemented our gelatin gel proton studies with ^{23}Na NMR relaxation measurements. Additional insight can be gained by comparing the proton transverse, longitudinal, and magnetization transfer rates at several spectrometer frequencies.

In this paper we therefore present a systematic multinuclear study of relaxation in gelatin gel over a range of water contents from 0 to 65% by weight and use the data to test the various hypotheses about the dynamic state of the system.

EXPERIMENTAL

Sample Preparation

Gelatins with variable water contents were prepared by drying a 70% water content gelatin (*11*). Warm water was added to the gelatin powder (PROLABO), which was left to dissolve at 58°C for 30 min. To prevent microbial growth, sodium azide (0.05%) was added to the gelatin. This also provided sufficient sodium for the Na^{23} NMR experiments described later. Gelatin gels were prepared by pouring the solution into a Petri dish to a height of 0.5–1 cm. It was then left to set in a sealed jar with a moisture content of 100%. Then, 0.5 cm cubes were cut from the gel and dried at 30°C in hermetically sealed jars containing saturated NaOH. They were removed at different times in order to obtain a broad range of water concentrations (≈0–70%, approximately). NMR tubes were filled to 3 cm height and sealed to avoid microbial development and exchange phenomena between the gelatin and the atmosphere. The moisture contents of the gelatin powder and of the prepared samples were measured by weight loss after drying for 24 h at 106°C. Results are expressed on a wet basis.

NMR Measurements

The measurements of the relaxation curves were carried out at 20°C on a Bruker 20 MHz Minispec pc120 with an audio filter bandwidth of 1 MHz and a phase sensitive detector. The measurements of the cross-relaxation flux were performed on a limited number of samples at the same temperature on an Oxford Instuments 20 MHz QP20 with a filter of 1 MHz. Longitudinal and transverse relaxation curves were also acquired at 100 and 300 MHz, respectively, on Bruker MSL 100 and MSL 300 spectrometers thermostated at 23°C.

For the 20 MHz proton measurements a 90°–*t*–90° pulse sequence, involving an FID and a progressive saturation, was used for simultaneous estimation of R_1, R_2^* slow relaxing component ($R^*_{2\mathrm{src}}$) and its initial amplitude ($M0_{\mathrm{src}}$) (*11, 13*). If FID_x is used as the amplitude of the signal x μs after the first 90° pulse, the slope of the plot of the logarithm of FID_x as a function of x, for x equal to 42 and 73 μs, may be considered equal to $-R_2\mathrm{src}$. $M0_{\mathrm{src}}$ may then be calculated as the exponential of the intersection at the origin. In the same way, if M_t represents the amplitude of the signal 11 μs after the 90°–*t*–90° sequence, the slope of the plot of the logarithm of $[(\mathrm{FID}_{11} - M_t)/\mathrm{FID}_{11}]$ as a function of t, for t equal to 7 and 70 ms, was considered equal to $-R_1$. Measurements were performed at 11 μs after the sequence and not at 70 μs because preliminary experiments had revealed that at 20°C, the relaxation can be considered monoexponential (the fast R_1 component only represents 5% of the total population). These times were chosen so as to give the greatest variation for the different water contents. In order to correct for variability in sample size, $M0_{\mathrm{src}}/\mathrm{FID}_{11}$ was calculated for each sample. In a second step, classical sequences such as CPMG for R_2 or inversion–recovery (I-R) for R_1 were used to validate the estimates obtained using the above sequences. R_1 was measured with an IR time delay ranging from 0.5 ms to 3 s. For the R_2, two CPMGs were used with 90–180 interpulse delays (τ) varying between 100 and 500 μs. The number of measurements was optimized to ensure sufficient points in the fast relaxing zone and a relatively short baseline.

Cross-relaxation rates were determined with the compensated Goldman–Shen sequence (*14, 15*) with a time delay of 50 μs so that the rapidly relaxing solid component was completely relaxed while leaving substantial signal in the mobile component. Variable contact times of 0.2 μs to 10 s were then used to monitor magnetization transfer. Longitudinal relaxation during the contact time was partly compensated by adding the signals acquired after phase cycling (*15*). Points were acquired between 12 and 14 μs (dwell time = 0.2 μs, 11 points) and between 50 and 60 μs (dwell time = 0.2 μs, 51 points) after the third 90° pulse in order to characterize both the growing solid and the decreasing liquid components. To improve the signal/noise ratio, the two sets of points were averaged.

The proton NMR measurements at 100 and 300 MHz were only carried out on six gelatin samples with water contents ranging from 5 to 65% water (wet basis). CPMG sequences with 90–180° pulse spacings varying between 100 and 200 μs and with points acquired every 1 or 2 echoes were used to acquire the transverse relaxation curves. For each sample, the sequence parameters were optimized to correctly characterize both the fast and slow relaxing components. For the water-poor samples, the reduced signal-to-noise was compensated by increasing the number of accumulated scans to 64. Longitudinal relaxation recovery envelopes were acquired using inversion–recovery sequences with 128 points and a step of either 10 or 25 ms, depending on the sample hydration.

^{23}Na NMR experiments were performed with a high-power broadband probe on a Bruker MSL 300 spectrometer operating at 79.387 MHz for sodium. The FID was measured with a dwell time of 17 μs for the water-rich samples (512 scans) and a dwell time of 4 μs for the water-poor samples (4096 scans). Relaxation times were determined by Lorentzian fitting of the sodium line-

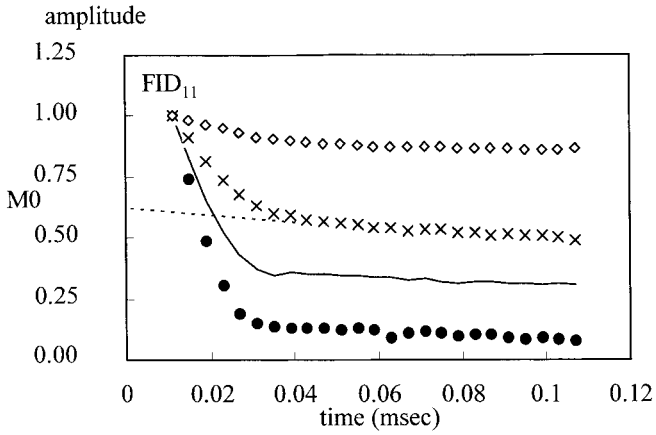

FIG. 1. Normalized amplitude of the FID curves for gelatins observed at 20 MHz and 20°C at different water contents (●: 4.93; −: 15.86; x: 20.1; ◇: 57.73%, wet basis). The extrapolated signal intensity for the slow relaxing component, $M0$, is indicated as well as the total signal intensity at 11 μs, FID_{11}.

shape. In theory, this is only an apparent transverse relaxation time because sodium has a spin number of $\frac{3}{2}$, so the signal should be biexponential with a ratio of 60:40, if all the sodium is NMR-visible, and the peaks would not be Lorentzian. In practice we were unable to detect any nonexponential behavior and the lineshape was well fitted with a single Lorentzian.

THE PROTON-EXCHANGE CROSS-RELAXATION MODEL

The proton exchange cross-relaxation model (*8, 9*) that has been developed for water-rich biopolymer systems will be briefly reviewed here to identify its limitations at lower water contents. The model assumes four proton pools, each associated with their own intrinsic proton transverse and longitudinal relaxation times. The first pool consists of bulk water whose motion is essentially unperturbed by biopolymer interactions. The second pool consists of hydration water, whose correlation times are lengthened by interaction with the biopolymer. Exchangeable gelatin protons make up the third pool, while the nonexchanging gelatin protons form the last pool. In the dilute regime there is fast exchange of water between the first two pools, i.e., between the bulk and hydration water, so on the NMR measurement time scale they can be considered as a single pool. The analysis of the various exchange processes in the dilute regime then proceeds as follows. Dipolar cross relaxation mechanisms are inoperative with transverse magnetization, so proton exchange between the water and exchangeable biopolymer protons provides the principal transfer mechanism. Moreover, spin diffusion between the biopolmer exchangeable and nonexchangeable proton pools is also nonexistent for transverse magnetization, so the nonexchanging proton pool appears as an isolated signal in the proton FID (*8*). Similar considerations are expected to apply in the low-water-content regime, except that at very low water contents the proton exchange rate is expected to become very slow on the NMR relaxation time scale so all transfer between the water and biopolymer pools should cease at sufficiently low water contents. The observation of fast and slow relaxation components in the FID (see Fig. 1) lends credence to this expectation.

The situation with the longitudinal magnetization is more complicated. In addition to proton exchange, secular dipolar cross relaxation can also transfer longitudinal magnetization between the water and biopolymer pools and permit spin diffusion between the various exchangeable and nonexchangeable gelatin proton pools. The effects of these exchange processes on longitudinal relaxation in the dilute regime has been described in previous work (*8*). The analysis of the low-water content regime, when proton exchange can be neglected, will be the subject of the next section.

TRANSVERSE ^{1}H AND ^{23}Na RELAXATION AT LOW WATER CONTENTS

Figure 1 shows the fast and slow decaying components in the free induction decay (FID) of concentrated and diluted gelatin gels. Although it is not possible to assign these components with certainty, we proceed on the hypothesis that the slow-relaxing component arises from hydration water, together with mobilized low molecular weight oligopeptides and possibly the extremities of gelatin chains. The fast-decaying component we assume arises from rigid gelatin protons. The ratio ($M0_{src}/FID_{11}$) of the amplitude of the slow relaxing component, $M0_{src}$, obtained by extrapolation to zero time, to the initial amplitude after 11 μs, FID_{11}, is a useful measure of the amount of the mobile component (or hydration water) and this ratio is

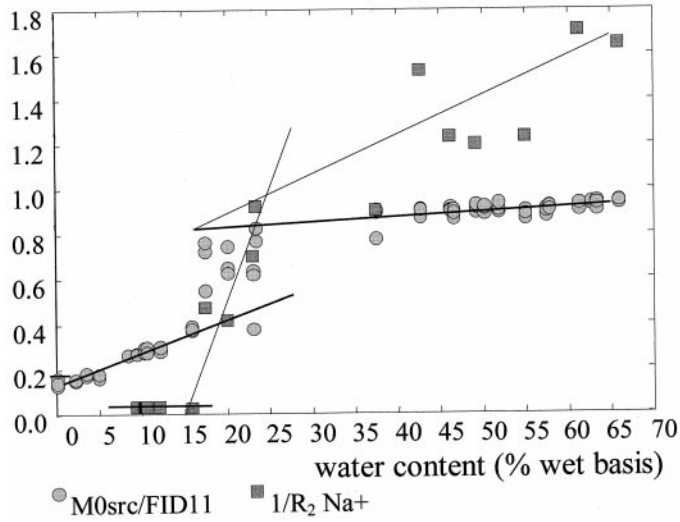

FIG. 2. Initial ^{1}H NMR signal amplitude of the slow relaxing protons divided by the amplitude of the FID signal at 11 μs (●: $M0_{src}/FID_{11}$) and sodium relaxation times (■: ^{23}Na $1/R_2$) as a function of the water content. A sudden change in slope is visible for both parameters in the 10–20% water content region.

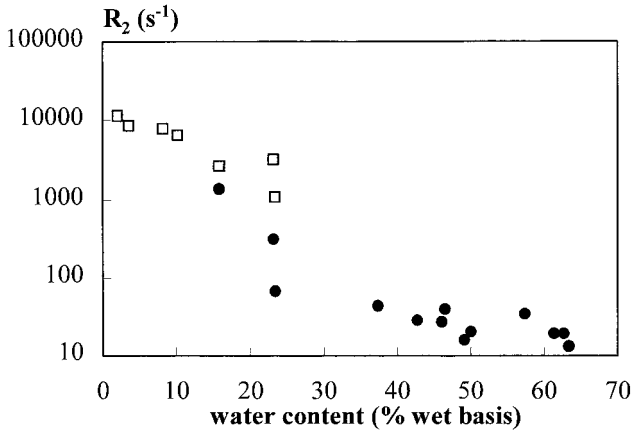

FIG. 3. Transverse relaxation rates (s^{-1}) of gelatin measured at 20 MHz as a function of water content. (□) from the FID; (●) from the CPMG sequence.

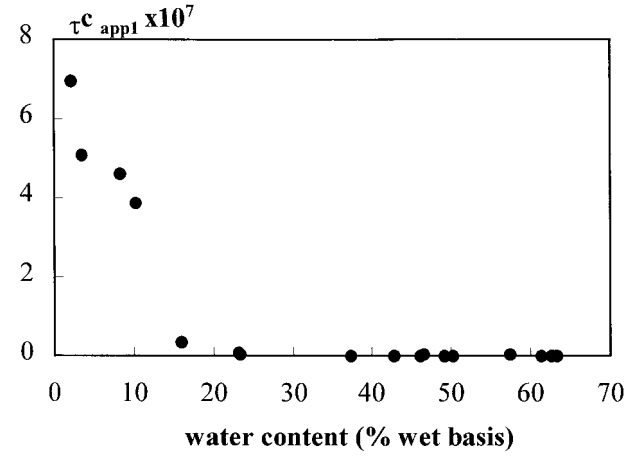

FIG. 4. Apparent correlation time τ_{capp1} calculated from the R_2 equation as a function of water contents of the gelatins. The bound water fraction η was taken as equal to 1 in the water content region 0–20% and estimated from Fig. 5 for higher moisture contents.

plotted as a function of water content in Fig. 2. This plot shows a clear discontinuity at water contents between 15 and 20% and, if our hypothesis is correct, could correspond to removal of multilayer water down to monolayer coverage. In other words, multilayer hydration water only begins to be formed at water contents exceeding ca. 15%. If so, dehydrating below 15% should remove progressively more strongly adsorbed water from the monolayer and should result in apparent increases in the transverse relaxation rate of the mobile component and in its associated correlation times. The amplitude drop of $M0_{src}/FID_{11}$ from 0.8 to 0.4 when decreasing water content could correspond to several phenomena such as water mobilization or solute mobilization. Figure 3 shows the dependence of the transverse relaxation rate, R_2, for the slowly relaxing component on water content, measured both from the FID and, at higher water contents, with the CPMG sequence. Once again a transition to higher values at water contents below 20% is apparent. In Fig. 4 we have analyzed this relaxation rate with a single correlation time model, according to the well-known equation

$$R_2 = 2\eta C/3\{J(0, \tau_c) + (5/3)J(\omega_0, \tau_c) + (2/3)J(2\omega_0, \tau_c)\} + (1 - \eta)R_{2w}, \quad [1]$$

where

$$J(\omega, \tau_c) = \tau_c/(1 + \omega^2\tau_c^2). \quad [2]$$

ω_0 is the proton Larmor frequency, η is the fraction of bound water molecules, and the dipolar coupling constant, C, is 2.5 10^{10} s^{-2} for water. R_{2w}, the relaxation rate for pure, bulk water, is close to 0.5 s^{-1}, so the term $(1 - \eta)R_{2w}$ can be neglected compared to the other terms. Figure 4 shows the dependence of the correlation time, τ_c, calculated from Eq. [1] on water content and shows an almost linear evolution as the water content is decreased below 20%. The bound water fraction, η, was estimated from our previous study on gelatin, which pointed out the analogy between the sorption isotherm and the dependence of the FID amplitude of the mobile water on water content (see Fig. 5, taken from Ref. *11*)). Below the inflection point B in Fig. 5, η can be considered to be unity, but at water contents above B, η is given as the ratio of DE/CE. It is interesting to note that the inflection point B occurs at 18.8% water, which corresponds to 0.23 g water per g dry gelatin, roughly the same as the amount of nonfreezing water in gelatin (*16*). This is consistent with the hypothesis that only bulk water, not adsorbed, multilayer water, can be frozen.

If our supposition that multilayer water only exists above ca. 15% is correct, one would expect that solutes, such as sodium

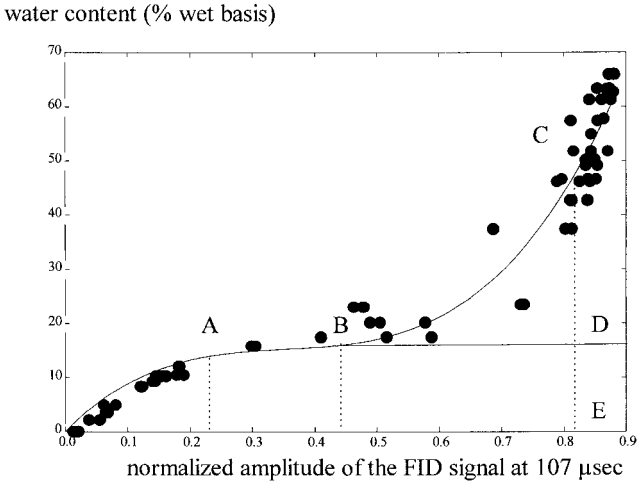

FIG. 5. Evolution of gelatin water content as a function of the normalized FID amplitude in the slow relaxing zone, measured at 107 μs.

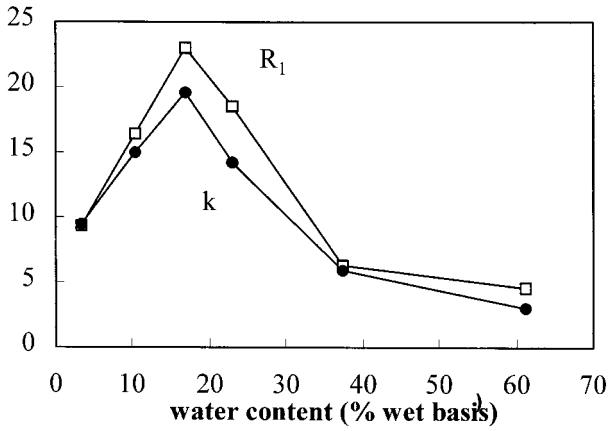

FIG. 6. Comparison of the longitudinal relaxation rates, R_1 (□), with the cross-relaxation rates, k_{cr} (●), at 20 MHz for gelatin as a function of water content.

ions, would only be mobilized at water contents exceeding this water content. To test this prediction, the dependence of the Na^{23} linewidth on water content in the gelatin gels was observed. The data is included in Fig. 2 and appears to be consistent with our supposition in that, at or below 15%, the sodium T_2 is too short to be measured reliably and above 15% there is a transition to much longer relaxation times. Above 20% the T_2 $(=1/R_2)$ increases with increasing water content as the amount of bulk hydration water increases and the mean lifetime of ions in the adsorbed water layer decreases.

LONGITUDINAL AND DIPOLAR CROSS RELAXATION

The dependence of the dipolar cross relaxation rate for longitudinal magnetization, k, measured with the Goldman–Shen sequence, on water content is plotted in Fig. 6 and shows an obvious maximum at a water content of ca. 15%. This maximum can be understood if it is noted that the observed rate, k, is the product $P|\sigma|$, where σ is the cross relaxation rate between a single proton pair, one proton belonging to hydration water and the other to a rigid protein chain; P is the number of hydrating water protons, proportional to the water content. Below 15%, the gelatin chains are in the rigid lattice regime and σ assumes a constant maximum value limited by spin diffusion within the protein lattice (*17*). Between 0 and ca. 15%, k is therefore given as $p\sigma_{max}$ and increases linearly with water content, reaching a maximum value at ca. 15%. Above 15% the pairwise cross relaxation rate begins to decrease because of the rapidly decreasing correlation time of the water (see Fig. 3). This decrease with decreasing τ_c follows from the form of the spectral density functions for σ (*8*), namely,

$$|\sigma| = (C^2/10)|J(0, \tau_c) - J(2\omega_0, \tau_c)|. \qquad [3]$$

A very similar explanation accounts for the dependence of the longitudinal relaxation rate on water content, which is included in Fig. 6. In the rigid lattice regime the intrinsic T_1 of the gelatin protons is expected to be quite long, possibly several seconds. In contrast, the more mobile hydration water adsorbed on the gelatin surface is expected to have a shorter intrinsic T_1. The longitudinal magnetization is therefore expected to relax by transfer to the hydration water, which acts as a relaxation sink for the gelatin longitudinal magnetization. The observation that the T_1 data parallels the k data in Fig. 6 suggests that the rate-limiting step in this relaxation process is the transfer of magnetization from the gelatin to water protons with a rate k so that $R_1 = ak$, where a is a proportionality constant. If the relaxation time of the water protons is shorter than that of the gelatin protons, one would, in general, expect to observe biexponential longitudinal relaxation. This is not, in fact, observed, presumably because of the low relative number of water protons.

Additional support for this interpretation is to be found from an analysis of the water correlation time calculated using the longitudinal relaxation rate. If, somewhat naively, we were to neglect cross relaxation and assign the observed R_1 to water, then, analogously to Eq. [1], the single correlation time model predicts

$$R_1 = 2\eta C/3[J(\omega_0, \tau_c) + 2J(2\omega_0, \tau_c)] + (1 - \eta)R_{1w}. \qquad [4]$$

An apparent correlation time can now be calculated from Eqs. [1] and [4] by fitting the ratio R_1/R_2 and neglecting the terms in $(1 - \eta)$. The result is plotted in Fig. 7 and shows a large discrepancy with the correlation time calculated using only the transverse relaxation rate, which does not involve dipolar cross relaxation (see Fig. 3). This strongly suggests that cross relaxation cannot be neglected and supports the original assumption

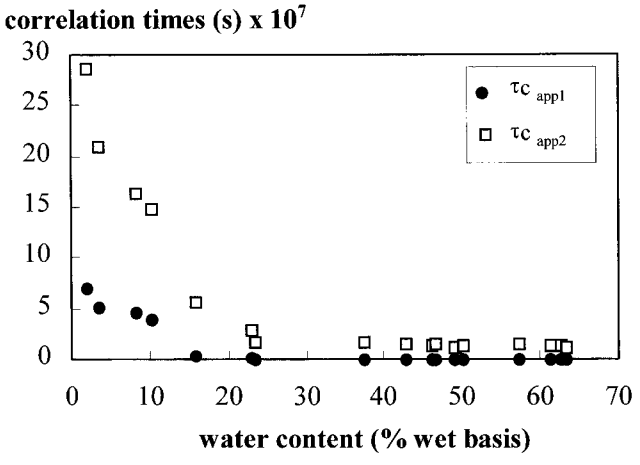

FIG. 7. Comparison betweeen the correlation time ($\tau_{c\,app1}$) calculated from R_2 Eq. [1] and the correlation time ($\tau_{c\,app2}$), obtained using both R_1 and R_2 as a function of the water content.

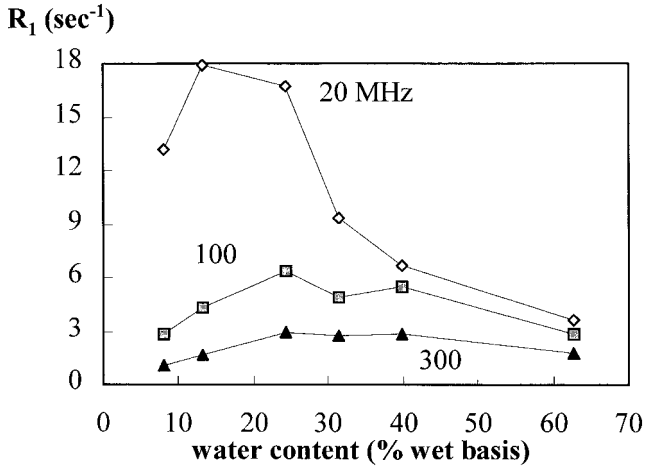

FIG. 8. R_1 at three different frequencies: 20 (◇), 100 (□), and 300 MHz (▲), as a function of water content.

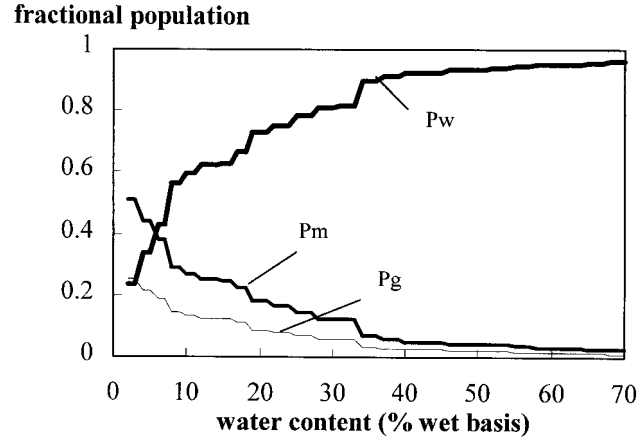

FIG. 9. Calculated dependence of the relative proton populations with water content in gelatin gels. P_w, exchangeable protons from water; P_m, nonexchangeable gelatin protons; P_g, exchangeable gelatin protons.

that the longitudinal relaxation rate is actually proportional to the dipolar cross relaxation rate. Additional confirmation is found in the dependence of the longitudinal relaxation rate on spectrometer frequency (Fig. 8). According to Eq. [3], $|\sigma|$, decreases with increasing spectrometer frequency, so that, if the previous arguments are correct, this should also result in a decrease in R_1 with increasing spectrometer frequency, which is obviously the case in Fig. 8.

It is instructive to estimate the relative proton populations from the known amino acid population of gelatin (*18*). Figure 9 shows the dependence of P_w, the proton fraction of water; P_m, the fraction of macromolecular nonexchanging protons; and P_g, the fraction of exchangeable gelatin protons, on water content. Not surprisingly, P_w increases with water content while P_m and P_g decrease. However, some interesting conclusions can be drawn by comparing the calculated proton populations in Fig. 9 with the change in the fraction of mobile protons obtained from Fig. 5. In the transition region between 15 and 20% water, the calculated proton fractions, obtained from Fig. 9, are compared in Table 1. At 20% water content the ratio $M0_{src}/FID_{11}$ is 0.8 and the sum ($P_w + P_g$) is 0.83. The near equality of these ratios shows that at 20% water content, all of the exchangeable proton pool is mobile. However, the ratios are quite different at 15% water content. The ratio $M0_{src}/FID_{11}$ has fallen sharply to 0.4 while the fraction of exchangeable protons ($P_w + P_g$) is still 0.75, which implies that only 53% of the exchangeable protons are still "mobile" and contribute to the slow-relaxing component of the FID. If we assume that proton exchange has effectively ceased on the NMR time scale at 15% water content, then the exchangeable gelatin proton pool, P_g, will be associated with the fast-relaxing gelatin proton pool, P_m. This leaves only the water proton pool, P_w, which is 0.63 at 15% water content. Because the mobile proton fraction is only 0.4, a fraction (0.63–0.4) of water is associated with the fast-relaxing "rigid" proton pool and not with the slow-relaxing "mobile" proton pool at 15% water content. This deduction is entirely consistent with the multilayer water model because the removal of multilayer water will increase the lifetime of the water molecules adsorbed at the protein binding sites, thus converting them from "mobile" to "solid-like" protons. The rigidity of the protein chains, and hence the correlation time of the adsorbed water, will also increase as the plasticization effect of multilayer water is lost. However, the figures in Table 1 show that the increase in mobile proton fraction between 15 and 20% cannot result solely from the mobilization of nonexchanging gelatin protons because their proton fraction, P_m, is too small and it does not change significantly between 15 and 20% water contents. In other words, these results contradict the hypothesis that the observed changes are caused entirely by matrix mobilization.

DISCUSSION

The first and most obvious conclusion of our analysis is the distinct transition occurring in the relaxation and cross relaxation rates at water contents of ca. 15%. This water content, we believe, corresponds to monolayer coverage of the gelatin chains, a conclusion that is consistent with our observation that the sodium NMR relaxation times also show a dramatic in-

TABLE 1
Population Proportions Estimated from Fig. 9, for Gelatins at 15% and 20% Water

Population	15% water content	20% water content
P_g	0.12	0.09
P_m	0.25	0.17
P_w	0.63	0.74

crease at water contents in excess of 15%, presumably because of their solvation in the multilayer water. The observation that the changes in the longitudinal water relaxation rate with changing water content parallel those of the cross relaxation rates strongly suggests that the rate-limiting step is transfer of longitudinal magnetization between the hydration water and the biopolymer. Comparison of the proton population fractions with the fraction of mobile and immobile protons shows that the fraction of slow-relaxing, mobile protons increases much faster than the calculated fraction based on water content alone. There could be various reasons for this. Adding water to the system increases the mobility of the solid matrix and therefore lengthens correlation times. However, there are insufficient gelatin protons to account for the observed increase in the mobile fraction. Proton exchange will become significant as multilayer water is introduced, and this will add the fraction of exchangeable gelatin protons to the mobile pool. But this is also insufficient to account completely for the increase in mobile fraction. Our analysis suggests that the main contributing factor is the increased mobility of water associated with the formation of hydration multilayers, caused by the fast exchange of water between bulk and adsorbed sites. It would be especially interesting to extend the frequency range of our measurements with a field cycling spectrometer and compare the proton, deuteron, and oxygen-17 relaxation dispersions. This approach has been especially fruitful in the dilute regime (*19*), but has yet to be extended into the low-water-content regime of concern in this article.

ACKNOWLEDGMENTS

The authors gratefully acknowledge financial support from the INRA (Institut National de la Recherche Agronomique). They also thank Michel Piot (INRA-LRTL, Laboratoire de Technologie Laitière, Rennes, France) for determining the gelatin amino acid composition.

REFERENCES

1. R. M. Brunne, E. Liepinsh, G. Otting, K. Wüthrich, and W. F. van Gunsteren, *J. Mol. Biol.* **231,** 1040 (1993).
2. G. Otting, E. Liepinsh, and K. Wuthrich, *Science* **254,** 974 (1991).
3. P. S. Belton, S. G. Ring, R. L. Botham, and B. P. Hills, *Mol. Phys.* **72,** 1123 (1991).
4. B. P. Hills, H. Tang, P. S. Belton, A. Khalik, and R. Harris, *J. Molec. Liquids* **75,** 45 (1998).
5. B. Halle, T. Anderson, S. Forsen, and B. Lindman, *J. Am. Chem. Soc.* **103,** 500 (1981).
6. T. O. Thomas and J. C. Leyte, *Mol. Phys.* **91,** 715 (1997).
7. A. M. Gill, P. S. Belton, and B. P. Hills, *Ann. Rep. NMR Spectrosc.* **32,** 1 (1996).
8. B. P. Hills, *Mol. Phys.* **76,** 489 (1992).
9. B. P. Hills, *Mol. Phys.* **76,** 509 (1992).
10. M. C. Vackier and D. N. Rutledge, *J. Mag. Res. Anal.* **2,** 311 (1996).
11. M. C. Vackier and D. N. Rutledge, *J. Food Chem.* **57,** 287 (1996).
12. M. C. Vackier, A. S. Barros, and D. N. Rutledge, *J. Mag. Res. Anal.* **2,** 321 (1996).
13. J. P. Monteiro Marques, D. N. Rutledge, and C. J. Ducauze, *Lebens.-Wiss. Technol.* **24,** 93 (1991).
14. M. Goldman, and L. Shen, *Phys. Rev.* **144,** 321 (1966).
15. K. J. Packer and J. M. Pope, *J. Magn. Res.* **55,** 378 (1983).
16. I. D. Kuntz, Jr., and W. Kauzmann, *Adv. Protein Chem.* **28,** 239 (1974).
17. H. T. Edzes and E. T. Samulski, *Nature* **265,** 521 (1977).
18. A. White, P. Handler, and E. L. Smith, "Principles of Biochemistry," p. 980, McGraw-Hill, London (1973).
19. B. Halle and V. P. Denisov, *Biophys. J.* **69,** 242 (1995).